ELSEVIER

Journal of Molecular Catalysis A: Chemical 119 (1997) 289–297

JOURNAL OF MOLECULAR CATALYSIS A: CHEMICAL

Dynamical simulations of the oxygen adsorption on the Ag(110) surface

Vittoria Isabella Pazzi, Gian Franco Tantardini *

Dipartimento di Chimica Fisica ed Elettrochimica, Università degli Studi di Milano, Via Golgi 19, I-20133 Milan, Italy

Received 4 June 1996; accepted 22 July 1996

Abstract

The study of the adsorption of oxygen on silver surfaces is particularly important because it is a fundamental step in the catalytic partial oxidation of ethene. This gas–surface system is characterized by physisorption at low temperature, molecular and dissociative chemisorption at higher temperatures, and by the presence of a subsurface state. Starting from the results of recent molecular beam experiments, a theoretical study of the dynamical aspects of the process was initiated within the framework of a quasi classical trajectory approach. The reactive scattering of an O_2 beam on the (110) surface of Ag was simulated by using a LEPS potential which accounts for the electronic charge transfer from the metal surface to the incoming O_2 molecule. The dependence of the initial sticking coefficient of O_2 on its translational and rovibrational energies, on the incidence angles of the beam, and on the surface temperature was investigated.

Keywords: Sticking; Chemisorption; Reactive dynamics; Computer simulations

1. Introduction

The dissociative adsorption of molecular oxygen on silver surfaces represents a very interesting subject both for theoretical and experimental studies, because of its importance in the catalytic partial oxidation of ethene [1]. In particular, the Ag(110) surface is the most investigated one owing to its high reactivity with oxygen which adsorbs on it in four different states: at surface temperature, T_s, below 40 K, the O_2 molecule is weakly bound in a physisorbed state; in the range 40 K $< T_s <$ 150 K, it is molecularly chemisorbed; for higher temperatures, it chemisorbs dissociatively, and a subsurface state is also detected.

In this work, we present the results of a preliminary study of the adsorption dynamics of an O_2 beam incident on the Ag(110) surface. First, the model potential and the classical dynamical method used in the rigid surface simulations are described. Then, an outline of the corrections introduced to account for the metal atom motion is given. Finally, we discuss the results obtained for the adsorption probability, with particular emphasis on the role played by the different energy components of the O_2 molecule and by the surface temperature.

2. The O_2–Ag interaction potential

The metal surface was initially assumed to be rigid, so that no energy exchange with the incident molecule was possible. The interaction of

* Corresponding author: Tel.: +39-2-26603278; fax: +39-2-70638129; e-mail: tant@rsl.csrsrc.mi.cnr.it.

1381-1169/97/$17.00 Copyright © 1997 Elsevier Science B.V. All rights reserved.
PII S1381-1169(96)00492-X

O_2 with the (110) surface of silver was described by a LEPS (London–Eyring–Polanyi–Sato) potential [2], which is a non-pairwise valence bond type potential, with correct asymptotic behavior. For a diatomic molecule AB and a surface S, it has the form:

$$V_{\mathrm{LEPS}} = Q'_{\mathrm{AB}} + Q'_{\mathrm{AC}} + Q'_{\mathrm{BD}} - \left[J'^2_{\mathrm{AB}} + J'^2_{\mathrm{AC}} + J'^2_{\mathrm{BD}} - J'_{\mathrm{AB}} J'_{\mathrm{AC}} - J'_{\mathrm{AB}} J'_{\mathrm{BD}} + 2 J'_{\mathrm{AC}} J'_{\mathrm{BD}} \right]^{1/2}$$

where $Q'_i = Q_i/(1 + \Delta_i)$, $J'_i = J_i/(1 + \Delta_i)$, Q_i and J_i are the Coulomb and exchange integrals of diatoms i = A–B, A–C, B–D (C and D are the projections of A and B onto the surface, respectively), and Δ_i are the Sato parameters which give flexibility to the potential, especially in the transition state region. The Q_i and J_i integrals appearing in V_{LEPS} are related to the singlet and triplet state energies of the diatoms i, as following ${}^1V_i = (Q_i + J_i)/(1 + \Delta_i)$, and ${}^3V_i = (Q_i - J_i)/(1 - \Delta_i)$.

For the O–Ag interaction (A–C and B–D diatoms, in V_{LEPS}), we used a Morse function for the singlet state, ${}^1V_{\mathrm{OAg}} = D_{\mathrm{OAg}}\{1 - \exp[\alpha_{\mathrm{OAg}}(z^{\mathrm{e}}_{\mathrm{OAg}} - z_{\mathrm{OAg}})]\}^2$, and an anti-Morse function for the triplet state, ${}^3V_{\mathrm{OAg}} = D_{\mathrm{OAg}}\{1 + \exp[\alpha_{\mathrm{OAg}}(z^{\mathrm{e}}_{\mathrm{OAg}} - z_{\mathrm{OAg}})]\}^2/2$ where D_{OAg} is the O–Ag binding energy, $z^{\mathrm{e}}_{\mathrm{OAg}}$ is the equilibrium height of O above the surface, and α_{OAg} is the range parameter. In order to make the interaction potential dependent on the lateral position of the O atom across the surface, with the periodicity and the symmetry of the fcc (110) surface, we used for D_{OAg} and $z^{\mathrm{e}}_{\mathrm{OAg}}$ the following functions of the (x, y) coordinates of the projection of the O atom on the (110) plane

$$D_{\mathrm{OAg}}(x, y) = D_0 + D_1 \cos \omega_x + D_2 \cos \omega_y + D_3 \cos \omega_x \cos \omega_y$$

$$z^{\mathrm{e}}_{\mathrm{OAg}}(x, y) = z_0 + z_1 \cos \omega_x + z_2 \cos \omega_y + z_3 \cos \omega_x \cos \omega_y$$

with $\omega_x = 2\pi x/a_x$, $\omega_y = 2\pi y/a_y$, where $a_x = 2.89$ Å and $a_y = 4.09$ Å are the (110) unit cell lengths. The range parameter, α_{OAg}, is related to the dissociation energy by the following expression $\alpha_{\mathrm{OAg}}(x, y) = \pi c \omega [2\mu/D_{\mathrm{OAg}}(x, y)]^{1/2}$, ω and μ being the vibrational frequency and the reduced mass of the O–Ag diatom, and c the speed of light.

The values of the parameters appearing in the atom–surface interaction potentials are determined, in general, starting from experimental data or ab initio results. For the O–Ag system, it is known that the oxygen atoms are preferably adsorbed on long-bridge (LB) sites, at equilibrium height $z^{\mathrm{e}}_{\mathrm{LB}} \cong 0.0$ Å [3] (we used the value $z^{\mathrm{e}}_{\mathrm{LB}} = 0.24$ Å), with vibrational frequency $\omega = 325\ \mathrm{cm}^{-1}$ [4]. For the binding energy of the O atom to the LB site, the value $D_{\mathrm{LB}} = 3.3$ eV, obtained from the adsorption heat of O_2 on Ag (1.5 eV), and the O_2 dissociation energy (5.12 eV), was used. For the other high symmetry sites (hollow, H; short bridge, SB; top, T), we used the values $D_{\mathrm{H}} = 3.1$ eV, $D_{\mathrm{SB}} = 1.7$ eV, $D_{\mathrm{T}} = 1.0$ eV, and $z^{\mathrm{e}}_{\mathrm{H}} = 0.65$ Å, $z^{\mathrm{e}}_{\mathrm{SB}} = 1.65$ Å $z^{\mathrm{e}}_{\mathrm{T}} = 2.17$ Å, which come from a fitting of a sum of O–Ag Morse potentials to the values of D_{OAg}, $z^{\mathrm{e}}_{\mathrm{OAg}}$, and ω for the LB site [5]. The parameters (D_0, D_1, D_2, D_3) and (z_0, z_1, z_2, z_3), were fixed by requiring that the functions $D_{\mathrm{OAg}}(x, y)$ and $z^{\mathrm{e}}_{\mathrm{OAg}}(x, y)$ had in LB, H, SB and T adsorption sites the values reported above. For the sake of comparison, we mention the results of two recent ab initio density functional calculations, with gradient corrections to local density approximation. The first set of calculations (plane wave pseudopotential [6]), based on the use of a 6 layer slab with 3×2 surface cell, gives the values: $D_{\mathrm{LB}} = 3.11$ eV, $D_{\mathrm{H}} = 3.14$ eV, $D_{\mathrm{SB}} = 2.75$ eV, and $z^{\mathrm{e}}_{\mathrm{LB}} = 0.59$ Å, $z^{\mathrm{e}}_{\mathrm{H}} = 0.60$ Å, $z^{\mathrm{e}}_{\mathrm{SB}} = 1.56$ Å, while for the T site a value between 1 eV and 2 eV has been estimated. The second set of calculations (tight binding [7]), with a 2 layer slab and a 3×2 surface cell, gives: $D_{\mathrm{LB}} = 2.93$ eV, $D_{\mathrm{H}} = 2.91$ eV, $D_{\mathrm{SB}} = 1.98$ eV, $D_{\mathrm{T}} = 1.74$ eV, and $z^{\mathrm{e}}_{\mathrm{LB}} = 0.55$ Å, $z^{\mathrm{e}}_{\mathrm{H}} = 0.66$ Å, $z^{\mathrm{e}}_{\mathrm{SB}} = 1.82$ Å, $z^{\mathrm{e}}_{\mathrm{T}} = 1.97$ Å.

The O–O interaction potential (A–B, in V_{LEPS}) was built starting from the experimental

evidence that the O atoms adsorb on the Ag surface in $(n \times 1)$ overlayer structures, with n decreasing with increasing oxygen coverage ($n = 7$ at low coverages). This behavior is attributed to electrostatic repulsion between negatively charged O atoms lying in the $\langle 1\bar{1}0 \rangle$ grooves, as found in ab initio calculations [6,7]. For the singlet state, we used a Morse potential ${}^1V_{OO} = D_{OO}(1 - \exp[\alpha_{OO}(r^e_{OO} - r_{OO})])^2$, with $D_{OO} = 5.12$ eV, $r^e_{OO} = 1.208$ Å and $\alpha_{OO} = 2.680$ Å^{-1} [8]. The triplet state was described by the following potential [5]: ${}^3V_{OO} = V_{\langle 1\bar{1}0 \rangle} \cos^2\phi + V_{\langle 001 \rangle} \sin^2\phi$, where ϕ is the angle between the projection of the O–O bond on the surface and the $\langle 1\bar{1}0 \rangle$ direction; $V_{\langle 1\bar{1}0 \rangle}$ and $V_{\langle 001 \rangle}$ are the anti-bonding potentials for O_2 oriented along the $\langle 1\bar{1}0 \rangle$ and $\langle 001 \rangle$ directions. For them, we used the expressions: $V_{\langle 1\bar{1}0 \rangle} = (qe)^2/r + a/r^3$, with $q = -0.4$, $a = 6.81$ eV Å^3, and $V_{\langle 001 \rangle} = V_0 \exp(-\beta r)$, with $V_0 = 81.6$ eV, $\beta = 2.0$ Å^{-1} [5]. The value used for the charge q is comparable to that obtained in ab initio calculations [9], which predict the O_2 molecule adsorbed on Ag(110) as $O_2^{-\delta}$, with $\delta = 0.9$.

In Fig. 1, we have drawn the two dimensional contour plot for one of the most favorable approaches (in our calculations, Δ_{OO} and Δ_{OAg} were not used, that is, $\Delta_{OO} = \Delta_{OAg} = 0$), with the O_2 center of mass moving along the perpendicular to the Ag surface through a LB site, and the O–O bond stretching parallel to the surface, in the $\langle 1\bar{1}0 \rangle$ direction. It is possible to note in the entrance channel the presence of a barrier ($A = 0.21$ eV), followed by a molecular chemisorption well ($B = -0.36$ eV), which is separated by a hill ($C = -0.070$ eV) from the dissociative well ($D = -1.16$ eV). From experiment [10], it is known that the molecular adsorption energy is 0.40 eV (to be compared with our value, 0.36 eV, point B in Fig. 1), and the barrier separating the molecular from the atomic well is 0.34 eV (the energy difference between points C and B in Fig. 1 is 0.29 eV). Ab initio calculations [6] give the values 0.50 eV and 0.47 eV when the O_2 center of mass is above the H site with the molecular axis parallel to the

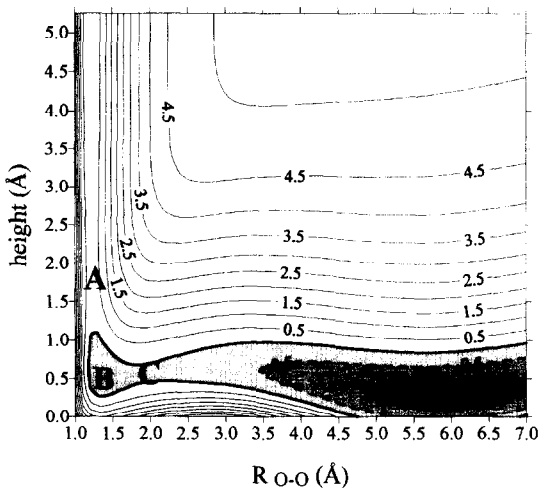

Fig. 1. Contour plot for O_2 moving on the vertical (z axis) through the long bridge site, with the O–O bond stretching parallel to the Ag surface in the $\langle 1\bar{1}0 \rangle$ direction; the vertical axis is the height of the molecular center of mass, and the horizontal axis is the O–O interatomic distance; energies (eV) are relative to free O_2 at equilibrium bond distance.

$\langle 1\bar{1}0 \rangle$ and $\langle 001 \rangle$ directions, respectively, and the value 0.10 eV when O_2 is on the LB site and aligned parallel to the $\langle 1\bar{1}0 \rangle$ direction.

3. Dynamical simulations

The adsorption dynamics of an O_2 beam on the Ag(110) surface was simulated by using the above potential in quasi classical trajectory calculations [2]. The 'experimental' conditions of the simulated beams were defined by the collision kinetic energy of the O_2 center of mass, E_{col}, the polar and azimuthal angles, Θ and Φ, defining the incident direction of O_2 at the surface, the quantum numbers v and j of the O_2 rovibrational state, and, for the non-rigid surface, the surface temperature, T_s. The remaining variables defining the initial conditions of each trajectory were treated as stochastic variables, and sampled according to their distribution laws. They are: (a) the coordinates, x_O and y_O, of the ideal point of impact of O_2 at the surface, in the absence of interaction; (b) the polar and az-

imuthal angles, ϑ and φ, defining the orientation of the O–O bond with respect to the incident direction at the surface; (c) the rovibrational phase, η; (d) the angle, χ, defining the orientation of the O_2 rotational angular momentum. The initial height of the O_2 center of mass above the surface was 10 Å.

The dissociative adsorption probability $P_a(E_{col}, \Theta, \Phi, v, j)$ was approximated by the ratio N_a/N between the number of trajectories, N_a, leading to adsorption and dissociation of O_2, and the total number of trajectories, N, in the simulated beam. The molecular sticking probability P_m was given by N_m/N, where N_m is the number of trajectories leading to chemisorption without dissociation. O_2 was considered molecularly chemisorbed after three complete oscillations of its center of mass above the surface. In non-rigid surface simulations, the validity of this criterion was checked by considering higher numbers of complete oscillations of the O_2 center of mass, and no significant changes in the results were found. In the rigid surface case, instead, we could not apply the same test because, as known, for sufficiently long integration times, the molecule or the atoms desorb from the surface. For the rigid surface, we computed $N = 1000$ trajectories for each set of initial conditions of the O_2 beam, so that the Monte Carlo standard error, $\lambda = [P_a(1 - P_a)/N]^{1/2}$, was lower than 0.02. The equations of motion were integrated using a predictor–corrector method, with time step $\Delta t = 0.02$ fs. For the non-rigid surface, we used $N = 300$ ($\lambda \leq 0.03$), and a Runge–Kutta–Gill integration method, with $\Delta t = 0.1$ fs. Some cases with $N = 1000$ were also considered, but the decrease of the statistical fluctuations was not followed by significant changes in the results.

4. Corrections for the non-rigid surface

It has been experimentally shown that a molecular chemisorbed state plays a basic role in dissociative chemisorption. Since the rigid surface approximation is inadequate to treat its effect, the motion of the Ag atoms was explicitly introduced in our simulations. To this aim, we used a cluster composed of four layers of 3×3 Ag atoms each, with periodic boundary conditions applied on the (110) plane. To describe the gas–surface interaction, we added to the LEPS potential, previously discussed, two further contributions: a first corrective term, V_{corr}, accounting for energy variations induced by displacements of the metal atoms from their lattice sites, and a second term, V_r, including the Ag–Ag interactions. V_{corr} has the form [11]:

$$V_{corr} = \sum_{\alpha} \left(V_{AB-\alpha} - V^0_{AB-\alpha} \right)$$

where α is a generic surface atom, $V_{AB-\alpha}$ is a three-body LEPS potential for the A–B–α system:

$$V_{AB-\alpha} = Q'_{AB} + Q'_{A\alpha} + Q'_{B\alpha} - \left\{ \left[\left(J'_{AB} - J'_{A\alpha} \right)^2 + \left(J'_{AB} - J'_{B\alpha} \right)^2 + \left(J'_{A\alpha} - J'_{B\alpha} \right)^2 \right] / 2 \right\}^{1/2}$$

and $V^0_{AB-\alpha}$ is the corresponding three-body LEPS potential when the α atom lies in its equilibrium position. The $Q'_{A\alpha}$ and $J'_{A\alpha}$ ($Q'_{B\alpha}$ and $J'_{B\alpha}$) integrals were computed using the O–Ag parameters for the LB site, that is, $D_{LB} = 3.3$ eV, $z^e_{LB} = 0.24$ Å, $\alpha_{LB} = 0.906$ Å^{-1}. V_r is a harmonic potential [12]:

$$V_r = \tfrac{1}{2} \sum_{\alpha i} \sum_{\beta j} \left(r_{\alpha i} - r^0_{\alpha i} \right) K_{\alpha i \beta j} \left(r_{\beta j} - r^0_{\beta j} \right)$$

where the force constants $K_{\alpha i \beta j}$ between atoms α and β (i, j indicate the x, y, z components), were obtained from the second derivatives of a sum of Lennard-Jones potentials [13].

According to a Langevin model [14], friction and random forces were also applied to the two innermost layer atoms of the cluster, in a direction normal to the surface plane, in order to account for the energy exchange with the bulk.

The complete set of the equations of motion are therefore:

$$m_g \ddot{r}_g(t) = -\nabla_g\left[V_{LEPS}(r_g) + V_{corr}(r_g, r_o)\right]$$

gas atoms

$$m_s \ddot{r}_o(t) = -\nabla_o V_r(r_o, r_i) - \nabla_o V_{corr}(r_g, r_o)$$

outermost layer atoms

$$m_s \ddot{r}_i(t) = -\nabla_i V_r(r_o, r_i) - \gamma \dot{r}_i(t) + R_i(t)$$

innermost layer atoms

where $-\gamma \dot{r}_i(t)$ and $R_i(t)$ are the friction force and the random force. To maintain the surface at any desired temperature, the two forces are balanced via the fluctuation–dissipation theorem, so that the width σ of the Gaussian distribution of the random force is related to the friction constant γ by the expression:

$$\sigma = (2\gamma m_s k_B T_s/h)^{1/2}$$

where m_s is the mass of the surface atom, k_B is the Boltzmann constant, T_s is the surface temperature, and h is the integration time step.

The initial conditions of the cluster were defined by considering the Ag atoms set to the crystal lattice sites, with velocities chosen from a Boltzmann distribution, at the surface temperature T_s.

5. Results and discussion

Recently, experiments have been performed with supersonic beams on the Ag(110) surface [15,16], in which the O_2 molecules are in the $v = 0$ state (owing to the rather large separation of the vibrational states), and populate the lowest rotational levels (as a consequence of the supersonic expansion). The results indicate that (a) the dissociative sticking probability, P_a, of O_2 on the (110) surface of Ag is much higher than that observed on the (111) surface; (b) P_a increases with O_2 collision energy, E_{col}, starting from a threshold at $E_{col} = 0.2$ eV, and reaching the maximum value of 0.5 at $E_{col} = 0.75$ eV; (c) P_a, decreases with increasing surface temperature. This behavior is interpreted by stating that the dissociative adsorption needs a molecular precursor state which is inhibited by high beam incident energies and high surface temperatures [15,16].

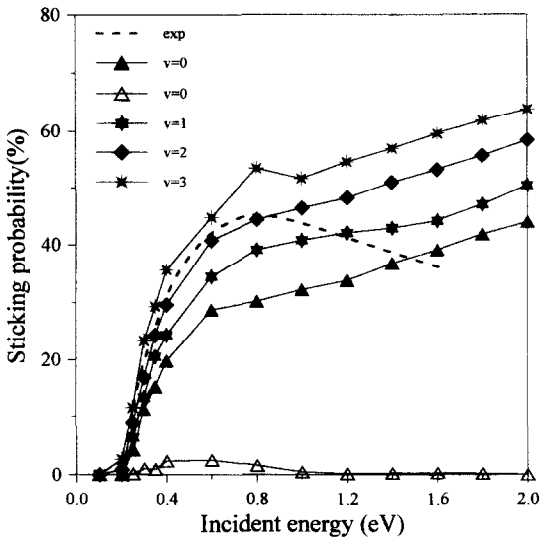

Fig. 2. Dissociative sticking probability, P_a, against O_2 collision energy, E_{col}, for the first four vibrational levels; $j = 0$, $\Theta = 0°$, $\Phi = 0°$; open symbol refers to molecular sticking probability; exp indicates the experimental curve [15], at surface temperature T_s = 300 K.

In our simulations of molecule–surface dynamics, we studied how the dissociative adsorption probability, P_a, is influenced by the translational, vibrational and rotational energy components of O_2, by the angles of incidence of the beam, and by the surface temperature.

In the first part of our study, the calculations were performed within the rigid surface approximation, which on one hand allows for significant savings of computer time, but on the other introduces too severe limitations for an adequate description of the molecular chemisorption process.

In Fig. 2, the curves representing the dependence of the dissociative sticking probability, P_a, from the initial collision energy of O_2, E_{col}, are drawn for different vibrational states of the molecule. Also reported in the figure are the experimental results at surface temperature T_s = 300 K [15], which can be compared with our

$v = 0$ curve. We can see that, for all the vibrational states we have analyzed, P_a increases with E_{col}, starting from a 0.2 eV threshold, as found experimentally. At low collision energies, the P_a versus E_{col} curves follow a trend similar to the experimental one, but at $E_{col} \cong 0.8$ eV they show a change of slope, whereas experimental results indicate the presence of a maximum. This different behavior is probably due to the absence of energy exchange between O_2 and the surface, which inhibits the molecular chemisorption, as shown in Fig. 2 by the low values of the molecular sticking probability, P_m. If one considers the results reported in Fig. 2 for the first four vibrational levels of O_2, it comes out that, at low values of E_{col}, the translational component of the molecular total energy is more effective than the vibrational energy in promoting dissociative chemisorption, but the trend is reversed at higher collision energies.

In Fig. 3 the results obtained for beams of molecules in different rotational levels of the ground vibrational state are drawn. At low collision energies, the dissociative chemisorption is inhibited by molecular rotation only in high rotational levels ($j = 30$). In any case, it seems that the role played by the rotational motion is somewhat diminished by the presence of the molecular adsorption well.

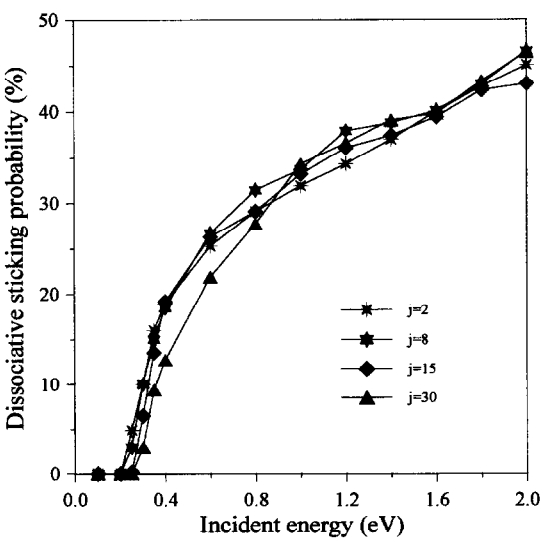

Fig. 3. Dissociative sticking probability, P_a, against O_2 collision energy, E_{col}, for different rotational levels; $v = 0$, $\Theta = 0°$, $\Phi = 0°$.

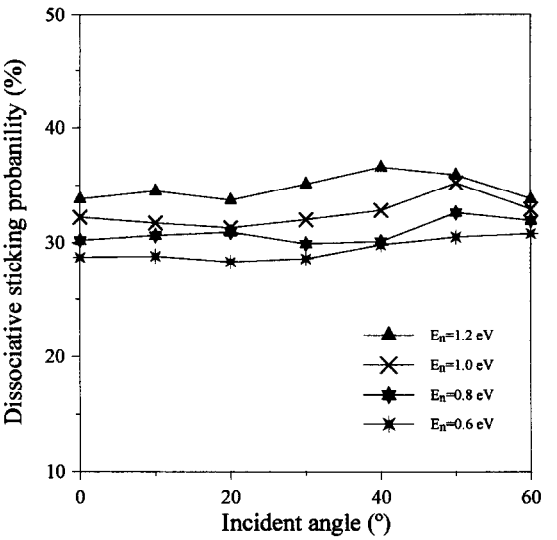

Fig. 4. Dissociative sticking probability, P_a, against O_2 incident polar angle for different normal collision energies, E_n; $v = 0$, $j = 0$, $\Phi = 0°$.

In Fig. 4, we report P_a against the incident polar angle Θ for different values of the normal component of the O_2 initial translational energy, $E_n = E_{col} \cdot \cos^2\Theta$, for the $\langle 1\bar{1}0 \rangle$ direction. It is evident that P_a approximately scales with normal energy, at least at incident angles lower than 40°. These results are in partial agreement with the experimental data, which show that P_a scales with a behavior which is intermediate between normal and total energy [15]. A quantitative measure of the dependence of P_a on Θ is given by the exponent n in the expression $P_a(E_{col}, \Theta) \cdot \cos\Theta = P_a(E_{col}, 0°) \cdot \cos^n\Theta$ [17]. We have found the values $n = 3.8$, 1.8, 1.5 for $E_{col} = 0.4$, 0.8, 1.2 eV, which suggest that the O_2 parallel momentum gets more important at higher incident energies.

It is also interesting to figure out the influence of the azimuthal angle of incidence on P_a. Fig. 5 shows the results obtained for two directions, the $\langle 1\bar{1}0 \rangle$, parallel to the grooves, and the $\langle 001 \rangle$, perpendicular to the grooves. Our results indicate that the dissociative chemisorption is easier in the $\langle 1\bar{1}0 \rangle$ direction than in the $\langle 001 \rangle$,

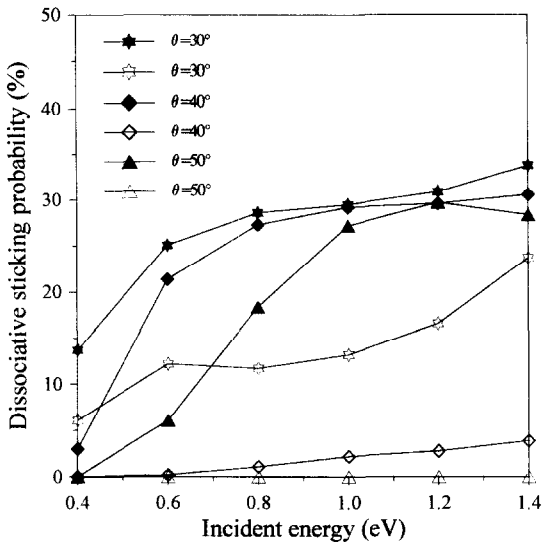

Fig. 5. Dissociative sticking probability, P_a, against O_2 initial collision energy, E_{col}, for different incident polar angles, in two azimuthal directions: $\langle 1\bar{1}0\rangle$ (filled symbols), and $\langle 001\rangle$ (open symbols); $v = 0$, $j = 0$.

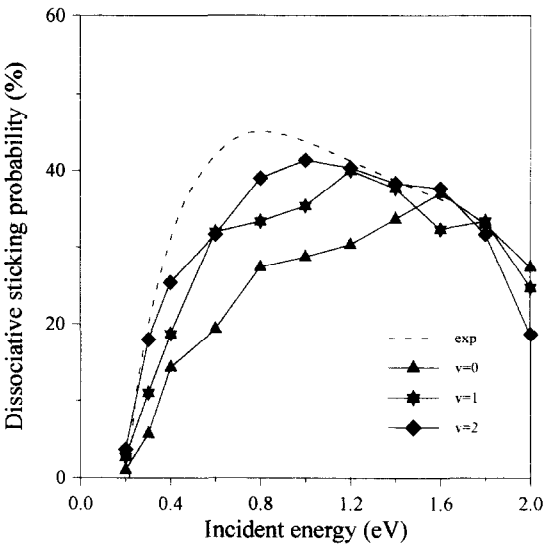

Fig. 6. Non-rigid surface: dissociative sticking probability, P_a, against O_2 collision energy, E_{col}, for the first three vibrational levels; $j = 0$, $\Theta = 0°$, $\Phi = 0°$; exp indicates the experimental curve [15], at surface temperature $T_s = 300$ K.

as opposite to experimental data [15,16]. The differences found for the two azimuthal directions are more relevant than those found experimentally, which are approximately $\Delta P_a \approx 5\%$.

In the second part of our calculations, the rigid surface constraint was removed, and preliminary results indicate that the silver atom motion plays a fundamental role both in the O_2 dissociative and molecular adsorption processes. In Figs. 6 and 7, the dependence of P_a and P_m on E_{col} is drawn for the first three vibrational states ($v = 0$, 1, 2). We can see in Fig. 6 that the dissociative sticking increases with E_{col}, showing a maximum in the P_a versus E_{col} curve, with a trend comparable to the experimental one. The location of the maximum moves toward lower values of E_{col} when the vibrational energy increases. For what concerns the molecular chemisorption (Fig. 7), it comes out that the P_m values are sensibly higher than those found in the rigid surface approach, confirming the role of the surface atom motion in stabilizing the molecular chemisorbed state, and the experimental hypothesis of a molecular precursor state mechanism. We can also see that P_m is strongly influenced by the vibrational energy, following a trend opposite to that found for P_a. This is a consequence of the fact that an increase of vibrational energy induces a weakening of the molecular bond, and consequently helps dissociation.

When considering the role of the surface temperature, we can see in Fig. 8 that the influence of T_s on the dissociative chemisorp-

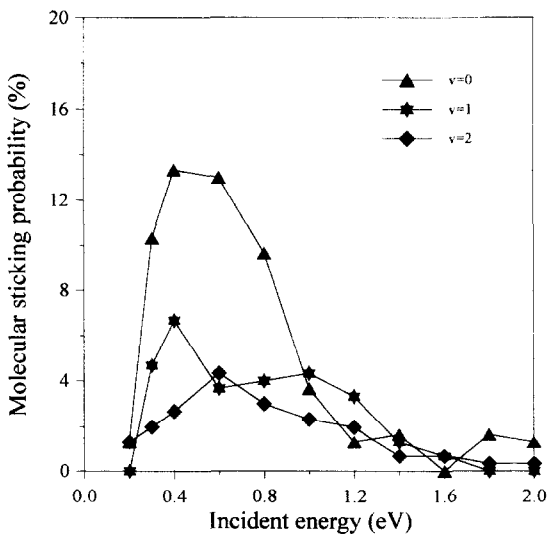

Fig. 7. Same as Fig. 6, for molecular sticking probability, P_m.

tion becomes evident only above 300 K, and for values of E_{col} higher than 0.4 eV. In those conditions, the curves show that P_a decreases with increasing T_s, and the maxima become more pronounced and shifted towards lower collision energies. This overall behavior has been observed in beam experiments, in which a remarkable decrease of the atomic sticking probability is found for $T_s > 200$ K [15]. On the contrary, the non-dissociative adsorption process seems to be scarcely influenced by the surface temperature as shown by the P_m curves in Fig. 9.

To conclude, from the results of our preliminary simulations, it comes out that it is of fundamental importance for the O_2–Ag(110) system to take into account the silver atom motion, because the molecule-surface energy exchange is crucial for a correct description of the molecular and dissociative chemisorption processes. Only in that case, we can obtain results which are in agreement with the experimental findings for what concerns the role played by the molecular chemisorption state. Other calculations are in progress, within the non-rigid surface approach, in order to gain a more detailed understanding of the dynamical behavior of this system.

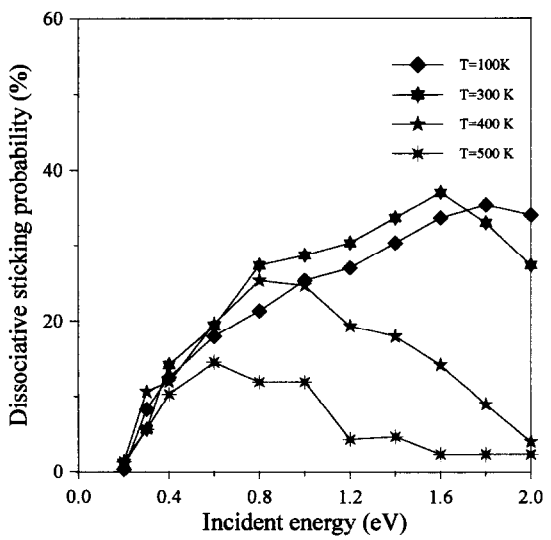

Fig. 8. Non-rigid surface: dissociative sticking probability, P_a, against O_2 collision energy, E_{col}, for different surface temperatures; $v = 0$, $j = 0$, $\Theta = 0°$, $\Phi = 0°$.

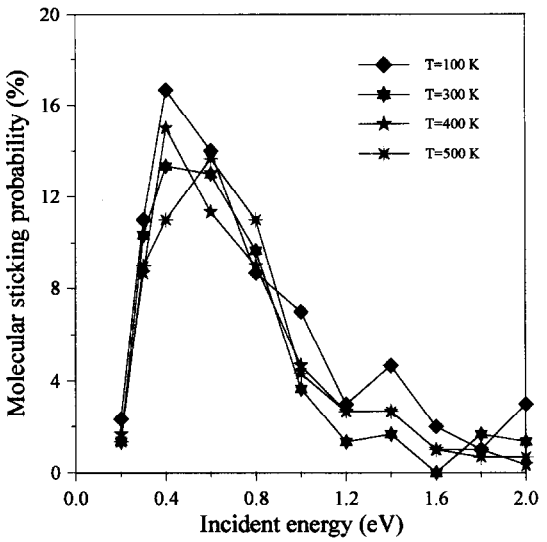

Fig. 9. Same as Fig. 8, for molecular sticking probability, P_m.

Acknowledgements

Work supported by Ministero dell'Università e della Ricerca Scientifica e Tecnologica, and by Consiglio Nazionale delle Ricerche. Part of the calculations were performed on the Convex HP META system of CILEA as a project of Centro di Modellistica Computazionale and on the CRAY T3D system of CINECA on account of a computational grant.

References

[1] R.A. van Santen and H.P.C.E. Kuipers, Adv. Catal. 35 (1987) 265.
[2] G.F. Tantardini and M. Simonetta, Surf. Sci. 105 (1981) 577.
[3] W. Heiland, F. Iberl, E. Taglauer and D. Menzel, Surf. Sci. 53 (1975) 383.
[4] M.A. Barteau and R.J. Madix, Surf. Sci. 97 (1980) 101.
[5] J.H. Lin and B.J Garrison, J. Chem. Phys. 80 (1984) 2904.
[6] P.A. Gravil, J.A. White and D. Bird, Surf. Sci. 352–354 (1996) 248.
[7] P. Philipsen and E.J. Baerends, private communication.
[8] K.P. Huber and G. Herzberg, Molecular Spectra and Molecular Structure IV. Constants of Diatomic Molecules, Van Nostrand Reinhold, New York, 1979.

[9] P.J van den Hoek and E.J. Baerends, Surf. Sci. 221 (1989) L791.
[10] C.T. Campbell, Surf. Sci. 157 (1985) 43.
[11] G.F. Tantardini and M. Simonetta, Chem. Phys. Lett. 87 (1982) 420.
[12] N.W. Ashcroft and N.D. Mermin, Solid State Physics (Saunders College, Philadelphia, 1976).
[13] A.E. DePristo, Surf. Sci. 141 (1984) 40.
[14] C. Lim, J.C. Tully, A. Amirav, P. Trevor and M.J. Cardillo, J. Chem. Phys. 87 (1987) 1808.
[15] A. Raukema, Ph.D. Thesis, Amsterdam (1995); A. Raukema, D.A. Butler and A.W. Kleyn, J. Phys. Condens. Matter 8 (1996) 2247.
[16] L. Vattuone, M. Rocca, C. Boragno and U. Valbusa, J. Chem. Phys. 101 (1994) 713.
[17] G. Comsa, in: Proc. 7th Intern. Vacuum Congr. and 3rd Intern. Conf. on Solid Surfaces, Vienna (1977) p. 1317.